Naval Research Laboratory

Washington, DC 20375-5320

NRL/MR/6750--04-8761

Temporally Resolved Langmuir Probe Measurements in LAPPS

DARRIN LEONHARDT
WILLIAM AMATUCCI
Charged Particle Physics Branch
Plasma Physics Division

GEORGE GATLING
SFA, Inc.
Landover, MD

April 12, 2004

REPORT DOCUMENTATION PAGE

Form Approved
OMB No. 0704-0188

1. REPORT DATE *(DD-MM-YYYY)*	2. REPORT TYPE	3. DATES COVERED *(From - To)*
April 12, 2004	Interim report	

4. TITLE AND SUBTITLE

Temporally Resolved Langmuir Probe Measurements in LAPPS

5a. CONTRACT NUMBER

5b. GRANT NUMBER

5c. PROGRAM ELEMENT NUMBER

6. AUTHOR(S)

Darrin Leonhardt, William Amatucci, and George Gatling*

5d. PROJECT NUMBER
67-7641-A4

5e. TASK NUMBER

5f. WORK UNIT NUMBER

7. PERFORMING ORGANIZATION NAME(S) AND ADDRESS(ES)

Naval Research Laboratory, Code 6750
4555 Overlook Avenue, SW
Washington, DC 20375-5320

SFA, Inc.
Landover, MD

8. PERFORMING ORGANIZATION REPORT NUMBER

NRL/MR/6750--04-8761

9. SPONSORING / MONITORING AGENCY NAME(S) AND ADDRESS(ES)

Office of Naval Research
800 North Quincy Street
Arlington, VA 22217-5660

10. SPONSOR / MONITOR'S ACRONYM(S)

11. SPONSOR / MONITOR'S REPORT NUMBER(S)

12. DISTRIBUTION / AVAILABILITY STATEMENT

Approved for public; distribution is unlimited.

13. SUPPLEMENTARY NOTES

SFA, Inc., Landover, MD

14. ABSTRACT

Electron beams efficiently ionize and dissociate gas, to form low temperature (<1.5 eV) high-density (10^{10}-10^{12}cm^{-3}) plasmas with low internal fields. These plasma sources have culminated in LAPPS, NRL's Large Area Plasma Processing System for surface modification of materials. Single Langmuir probes were constructed and used to determine global plasma parameters (electron temperature, density, and plasma potential) in modulated plasmas generated by high-energy (2 keV) electron beams. This work describes in detail the construction of probes, applications of probes in modulated systems and magnetic fields, data acquisition, and data analysis used in the study of electron beam generated plasmas.

15. SUBJECT TERMS

Langmuir probes; Modulated plasmas; e-beam generated plasmas

16. SECURITY CLASSIFICATION OF:			17. LIMITATION OF ABSTRACT	18. NUMBER OF PAGES	19a. NAME OF RESPONSIBLE PERSON
a. REPORT	b. ABSTRACT	c. THIS PAGE			Darrin Leonhardt
Unclassified	Unclassified	Unclassified	UL	28	19b. TELEPHONE NUMBER *(include area code)* (202) 767-7532

Standard Form 298 (Rev. 8-98)
Prescribed by ANSI Std. Z39.18

CONTENTS

TEMPORALLY RESOLVED LANGMUIR PROBE MEASUREMENTS IN LAPPS

D. Leonhardt, G. R. Gatling[†] and W. E. Amatucci

Plasma Physics Division, Code 6750
Naval Research Laboratory, Washington, DC

Abstract

Electron beams efficiently ionize and dissociate gas, to form low temperature (< 1.5 eV) high-density (10^{10}–10^{12} cm^{-3}) plasmas with low internal fields. These plasma sources have culminated in LAPPS, NRL's Large Area Plasma Processing System for surface modification of materials. Single Langmuir probes were constructed and used to determine global plasma parameters (electron temperature, density and plasma potential) in modulated plasmas generated by high-energy (2 keV) electron beams. This work describes in detail the construction of probes, applications of probes in modulated systems and magnetic fields, data acquisition, and data analysis used in the study of electron beam generated plasmas.

1. INTRODUCTION

Langmuir probes have been used in plasma environments since the 1920s[1] and there have been numerous reviews[2,3,4] on the theory and analysis of probe data. This work is therefore not a review of general probe theory but the implications and consequences of using a Langmuir probe in modulated, electron beam (e-beam) generated plasmas. Standard orbital motion-limited theory (OML) is applied, which

---

[†] SFA, Inc., Landover, MD

Manuscript approved March 19, 2004.

considers the probe as non-perturbative to the plasma. In other words, the probe is small compared to the sheath dimension, which is characteristically given by the electron Debye length[5], λ_D. Also, to allow a complete analysis of the data the plasma electron energy distribution is considered to be a single Maxwellian distribution. As shown in this paper, the validity of this assumption is supported by the data. Issues concerning probe surface contamination, electronics, computer controlled data acquisition/analysis, and the use of these probes in magnetic fields are addressed.

2. EXPERIMENTAL DESIGN

a. Electron Beam Production

A sheet of electrons produced by a linear hollow cathode formed the electron beam (e-beam) generated plasmas. A –2000 V pulse was applied to the cathode to produce a uniform e-beam (~ 0.1 mA/cm^2), which was collimated by an axial 165 Gauss magnetic field. A cross section of the hollow cathode source is shown in Fig. 1. In these

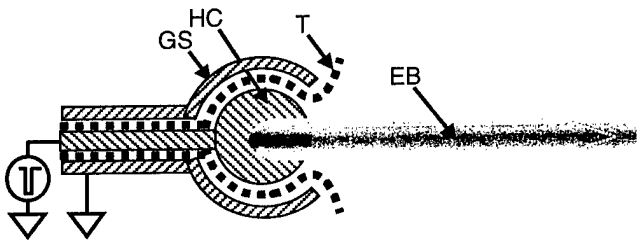

Figure 1 Cross sectional view of linear hollow cathode e-beam source. Labelled components are: ground shield (GS), hollow cathode (HC), Teflon® insulation (T), and electron beam/plasma (EB).

systems, cathodes were constructed from a variety of metals (brass, stainless steel) and insulators (Teflon®, Macor®) with similarly constructed support structures. Hollow cathode discharges were produced in grooves 1 cm wide by 1 – 1.5 cm deep and a variety

of lengths (15 – 50 cm). The e-beam is formed by secondary electrons emitted from the cathode surface and accelerated out of the groove due to the large negative potential. The output beam was skimmed by a slotted metal plate (grounded anode) located 5 - 10 cm downstream. The slot in this anode was the same dimensions of the cathode groove and was considered the cross section of emergent e-beam.

b. Langmuir probe construction

Probes were constructed from alumina (ceramic) and stainless steel tubes (hypodermic tubing) for rigidity and robustness. A complete table of specific materials and sources is listed in Appendix A. The inner insulator was a 1.6 mm diameter ceramic with four 0.4 mm bores, which housed the necessary wires. Two thoriated tungsten wires (0.13 mm diameter) were used for probes and a 'hairpin' of resistive wire (0.26 mm diameter, 6.5 Ω/ft) was used as a heater element. The ceramic was typically notched at the end to accommodate the bend in the heater wire, then filled in with ceramic paste. One tungsten wire probe protruded 2 mm out of the end of the ceramic, which provided a cylindrical probe of area approximately 4.9×10^{-3} cm^2. Another probe was constructed from a 3-4 mm length of metal hypodermic tubing that fit snugly over the ceramic tube with an area of 0.28 cm^2. This probe was mounted 5-6 mm from the end of the ceramic by the other tungsten wire, which was run through a cut in to one of the ceramic tube bores from the outside, then spot welded to the outer surface of the metal tube. By mounting two probes of largely different areas, plasmas with high and low electron densities (i.e. ion-ion plasmas) could be studied. Approximately 20 mm back from the larger probe, the remainder of the ceramic tube was covered by additional metal tube to

provide a local ground reference. Another alumina tube then covered the ground shield to prevent conduction of plasma current, which would otherwise disturb the plasma. A diagram of the probe assembly is shown in Fig. 2.

Connections to these wires were made at the other end of the 4-bore tube by either crimping small beryllium copper pins and sockets or spot welding. Varnished copper magnet wire or Teflon® insulated stranded hook-up wire was run from the probe assembly to the vacuum feed through flange, to minimize resistance and maximize current capability in the assembly.

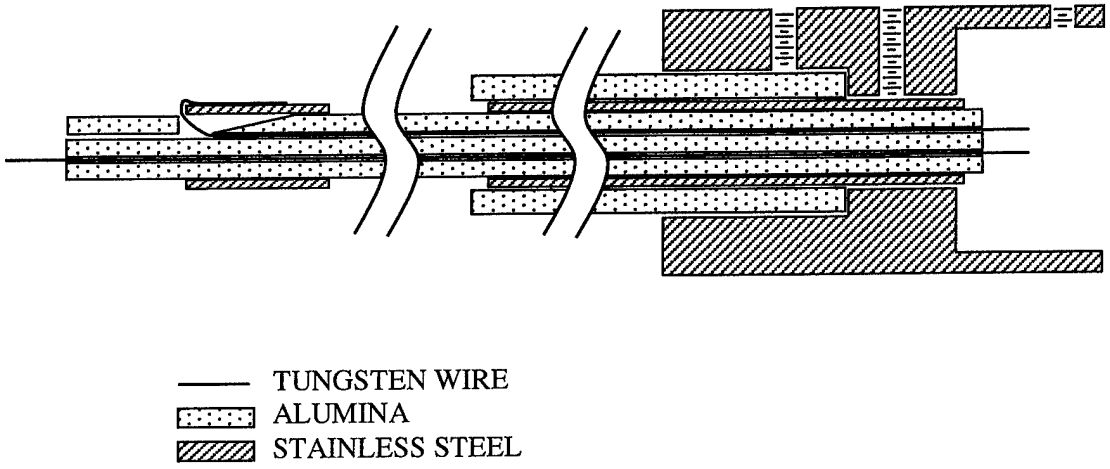

Figure 2 Mechanical construction of Langmuir probe. Set screws were used in stainless steel holder (right side of assembly) to hold parts in place. Heater element is not shown.

c. Probe wiring and electronics for data collection

Initial data collection was carried out with the standard wiring arrangement, shown in Fig. 3a. A variable voltage source (constructed with batteries and potentiometer) was used to apply a bias voltage (V_{bias}) to the probe in the plasma, and the current collected by the probe was measured through a load resistor, R_L ($<< 1M\Omega$). The voltage drop (V_L) across R_L was recorded with a digital oscilloscope (1 MΩ input

impedance) to correlate with the plasma on/off times of the modulated plasmas. This simple circuit was eventually replaced with the isolated amplifier[6] circuit shown in Fig. 3b, which significantly decreased noise pick-up in the measurements. The notch filter shown in Fig. 3b is a 2 pole low-pass Butterworth filter with a 50 kHz bandwidth to remove the 500 kHz carrier frequency of the ISO122.[7]

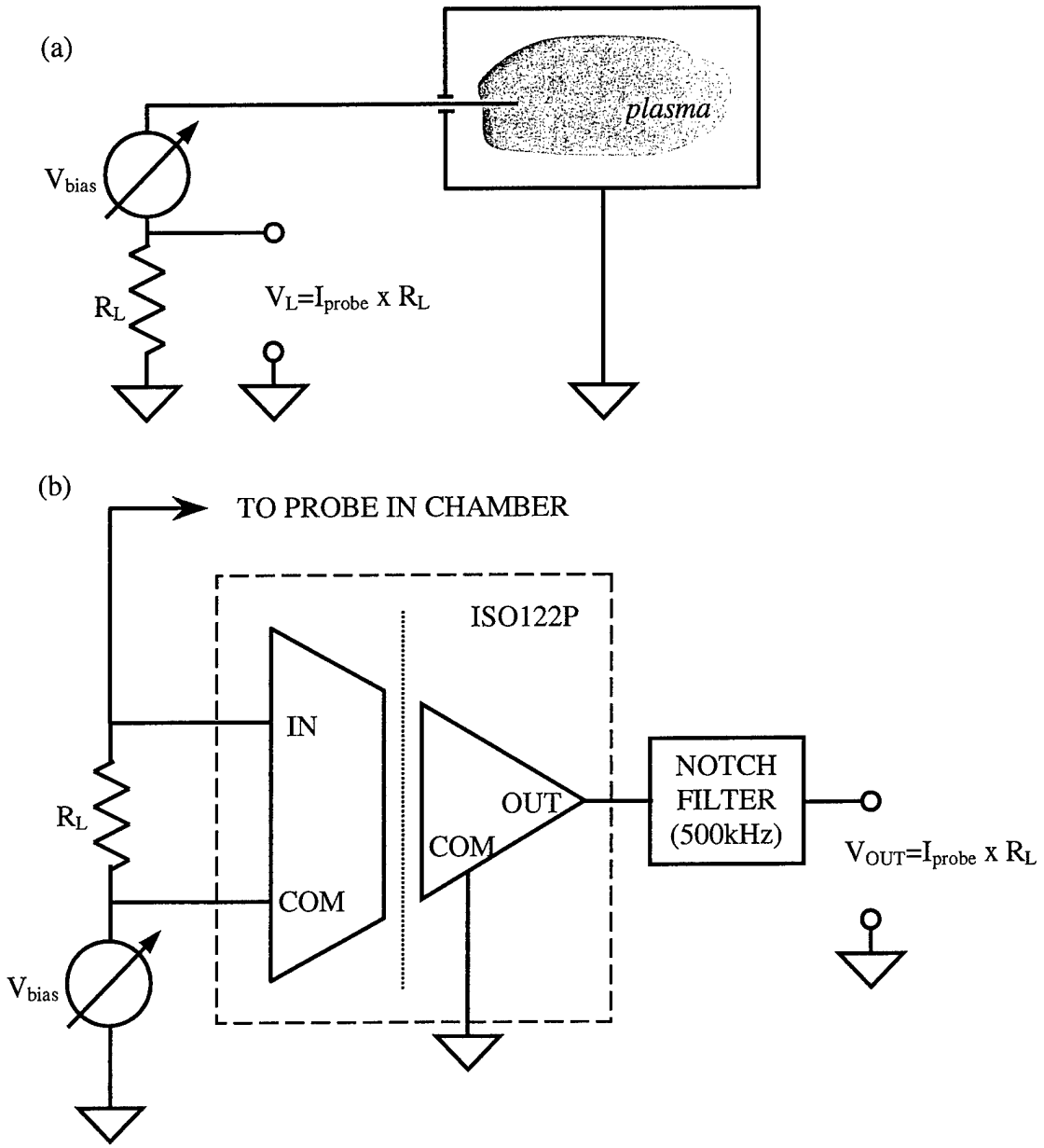

Figure 3 (a) Initial and (b) refined circuits used for Langmuir probe measurements.

d. Data collection and analysis

Langmuir probe I-V characteristics were created by plotting the measured probe current versus the applied bias voltage at various times with respect to the plasma pulse. Typically, 500 time divisions were used for temporal resolution at each bias voltage. Due to the large amount of data being collected for each I-V characteristic, the systematic collection of data evolved significantly during this work. Initially, the digital oscilloscope was used to manually collect individual probe current files at each bias voltage. This cumbersome technique was replaced by a system of boxcar averagers (Stanford Research SR250) that allowed direct acquisition of I-V characteristics in 3 μs windows, averaged over many plasma periods as the bias voltage was slowly scanned. The boxcars were connected to a computer interface module (Stanford Research SR245) that also provided an analog voltage for the bias voltage. This interface module was controlled by a LabVIEW™ code to scan the probe bias voltage then read, convert, and store each boxcar output signal in a columnar ASCII format.

Although the speed and efficiency at which data was collected and analyzed had been greatly increased, the few available boxcars (5) and their inherent baseline drift limited their usage for probe data acquisition. The boxcar system was replaced by a LabVIEW™ controlled system analogous to the original manual system. The LabVIEW™ program controlled the probe bias voltage, oscilloscope data collection and file storage to allow rapid data viewing. This program could control various bias voltage sources (Stanford Research SR245, Keithley 2400) and digital oscilloscopes (Tektronix TDS640/460) to measure the probe current. The system stepped the probe bias voltage in

discrete intervals and collected the temporally varying probe current; current averaging was also done by the oscilloscope over multiple periods to improve the data S/N ratio. Program inputs were the bias voltage intervals, number of plasma cycle averages, oscilloscope scaling ramp (for maximum sensitivity), voltage-to-current conversion, and an active data baseline subtraction. For an entire probe bias voltage scan, the temporally-resolved current measured at each voltage step was stored sequentially in a master ASCII data file. These data files were approximately 2 MB in size, for typical applied voltages (-10 V to +10 V in 0.05 V steps) and standard time resolutions (500 points/trace). The program also generated additional documentation and raw data files. The front panels of the LabVIEW™ program are shown in Fig. 4.

A LabVIEW™-driven data analysis routine that was used to determine the plasma parameters of electron temperature (T_e), plasma potential (V_{plasma}), floating potential (V_{float}), and electron density (n_e) also experienced several iterations. However, the basic mechanics[11] of the routine remained fundamentally the same. The plasma potential, V_{plasma}, was first determined from the maximum in the derivative of the I-V characteristic. The probe current data was then fit up to V_{plasma} with a function of the form $I(V) = a + bV^{\gamma} + c[\exp(\varphi/T_e)]$, where $\varphi \equiv V_{bias} - V_{plasma}$. The first two terms model the ion portion of the trace while the third term models the electron current. The exponent γ depends on the effective geometry of the probe (0.5 for a cylinder and 1 for a sphere) and the constants a, b and c are all parameters used to fit the data. The prefactor c is the electron saturation current to the probe, given by $en_eA(kT_e/2\pi m_e)^{1/2}$, where e is the electron charge, A is the probe area, k is Boltzmann's constant, and m_e is the electron mass. Values of a, b, and c are found for a series of T_e values, with the best combination

of values being the set that minimizes the error between the data and the fit. With the best c and T_e values, the electron density is finally calculated from the expression for c given above.

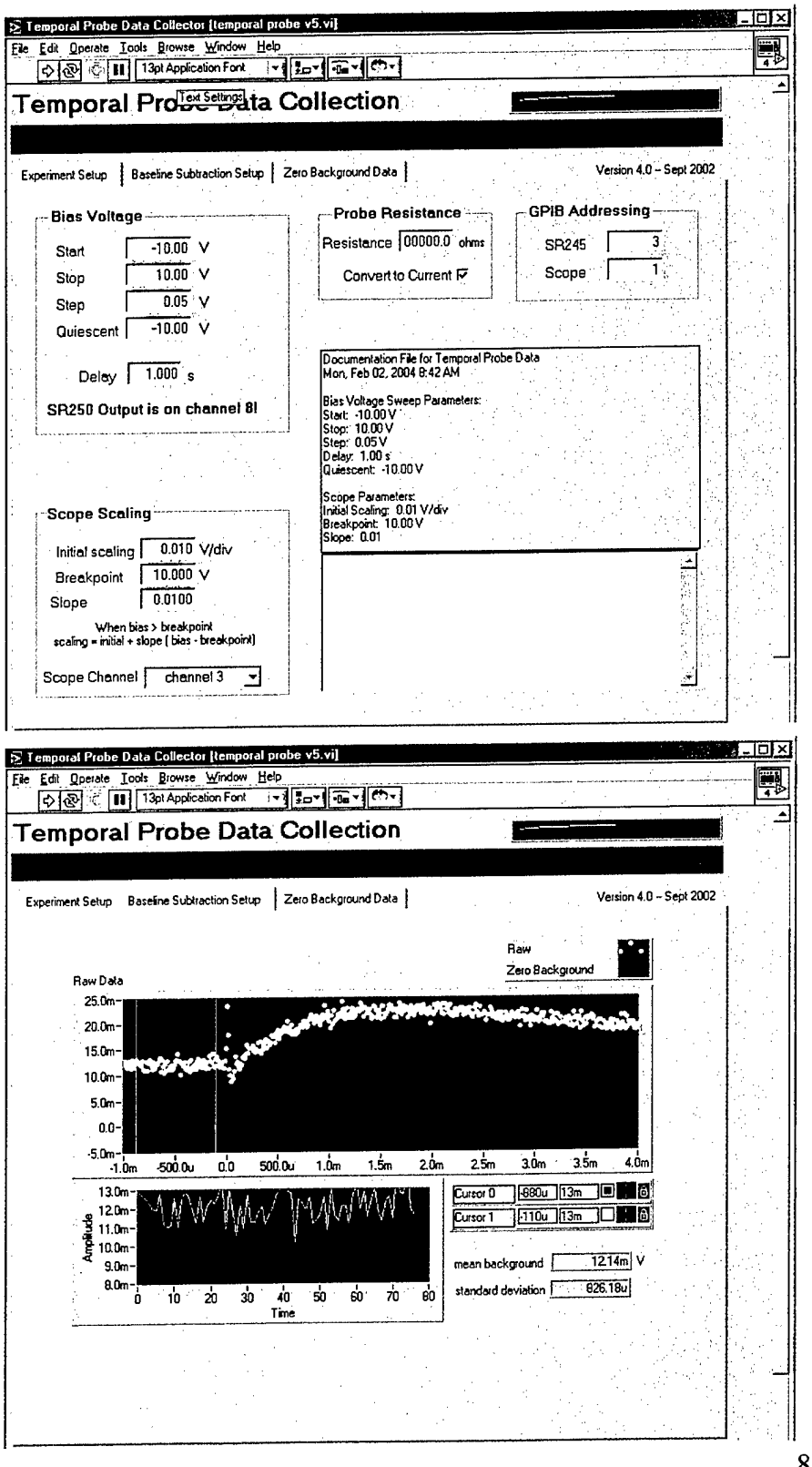

Figure 4 Data collection program front panels. (Top) Probe bias voltage scan and parameters and (bottom) background subtraction.

The final active version of the probe data analysis program (Langmuir Analysis.vi) could read and analyze the entire 2 MB data file. User inputs allowed the program to automatically compute the plasma parameters or compare a number of consecutive time intervals to reduce spurious results in the plasma parameters. The front end of this program also operated as a single trace analysis routine. This allowed the user to choose a specific time and adjust the plasma potential and/or electron temperature to obtain results if those produced by the automatic analysis did not produce a satisfactory fit to the data. Figure 5 shows the front panel from this batch analysis routine. The 'Active Trace' selection refers to the I-V trace shown in the plot on the right of the panel, with the number in the box being the time of the trace in seconds. The plasma parameters are plotted in the lower portion of the panel for the entire data file, with the 'Active Trace' being marked by the vertical cursor. The abundance of noise, particularly in T_e, was primarily concentrated in the plasma off times and was due to the fact that the program calculated a solution for all times in the given data file whether or not there was plasma.

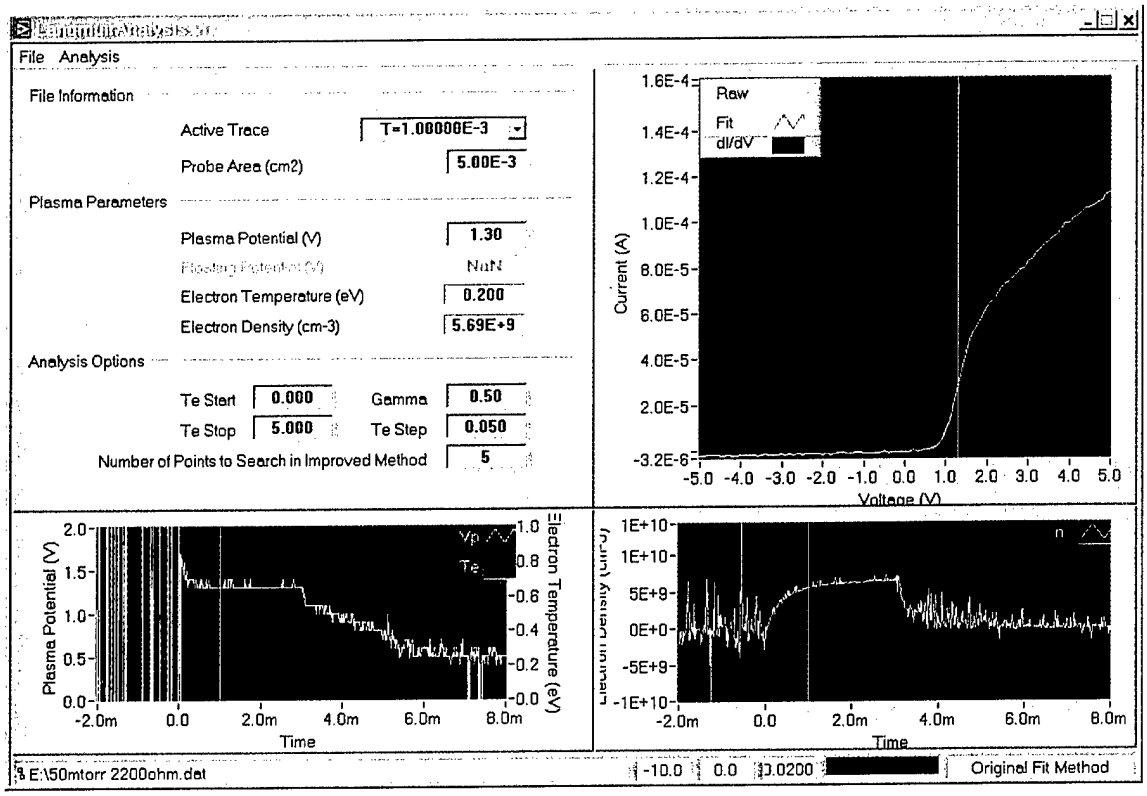

Figure 5 Front panel of "Langmuir Analysis.vi" used in batch data analysis.

3. DATA AND RESULTS

Probe I-V characteristics were taken in a variety of systems. The major obstacles that had to be overcome are illustrated in this section. These obstacles were probe contamination, circuit response time, and efficient data acquisition/analysis to achieve reproducible results in the various modulated LAPPS systems. In all cases, probe currents were kept small to prevent a significant voltage drop from the applied bias voltage.

a. Probe contamination[8]

Probe contamination was probably the largest obstacle to recognize and overcome. In these modulated plasma environments, the probe could not be actively cleaned by ion or electron bombardment reliably, since acquisition of the complete set of

I-V characteristics took 10 - 30 minutes. This meant that the probe surface was constantly changing, adsorbing many monolayers of background gas (and in most cases, contaminants) during any single I-V characteristic. The most effective method found to record reproducible I-V traces was to heat the probe. An experimentally determined[9] progression through the surface changes is shown in Fig. 6, where the probe I-V traces are plotted for various heater currents for the same time during the plasma pulse. This data was taken with the boxcar averagers and also shows the inherent baseline offset associated with these devices. The I-V characteristics showed a significantly steeper slope (lower T_e) and shifted knee (V_{plasma}) in the transition region as the heater current (or probe temperature) increased. The calculated plasma parameters from these I-V characteristics, approximate probe temperatures, and a comparative 'goodness of fit' to a single Maxwellian electron energy distribution are listed in Table I.

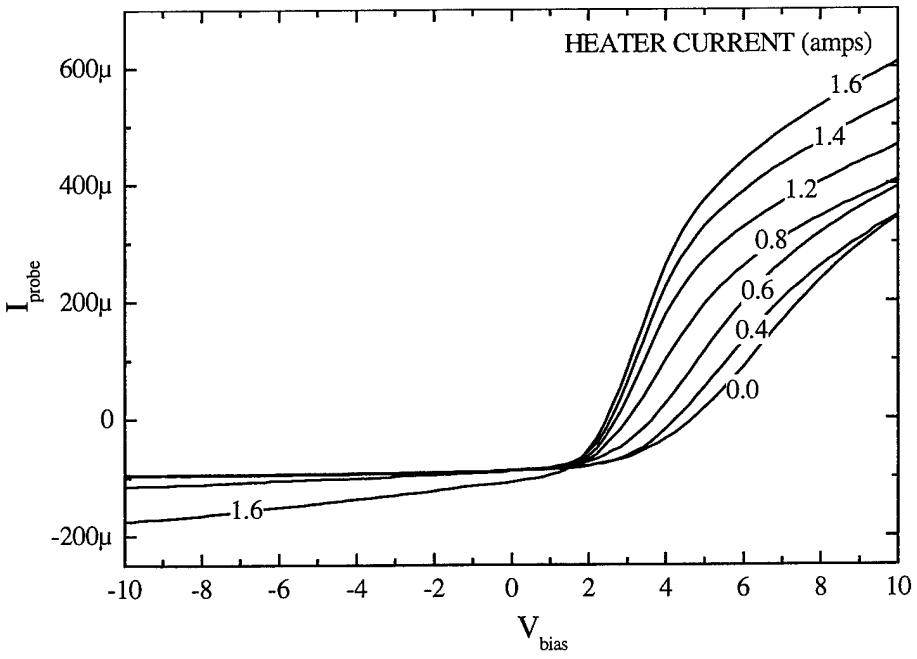

Figure 6 I-V characteristics at various probe temperatures (heater currents).

Table I Plasma parameters, approximate probe temperatures and comparative fit results for I-V traces shown in Figure 6.

Heater current (A)	Approx. Temp. (°C)	T_e (eV)	V_{plasma} (V)	n_e ($\times 10^{11}$ cm^{-3})	Fit Comments
0	18	1.83	6.28	3.4	Poor
0.4	61	1.83	6.08	4.1	Poor
0.6	122	1.35	4.67	3.4	Better
0.8	182	1.05	3.87	3.9	OK
1.2	304	0.80	3.37	4.3	Good
1.4	364	0.75	3.37	5.0	Good
1.6	425	0.85	3.47	5.5	OK

b. Probe temporal response due to bias voltage power supply

A fast temporal response of probe system electronics was necessary to study the plasma evolution and afterglow. A broad range of results was obtained with standard laboratory power supplies, which made it difficult to confirm whether the physics of the system or the diagnostic were dominating the measurements. Specifically, the current slew rate of the probe bias supply had to be fairly high to match the rapidly changing probe currents from the modulated plasma. Additional electronic components (such as amplifiers) typically have very fast response times and were not considered a limiting factor in these systems.

Figure 7 shows the electron saturation signals from a heated ($\approx$ 490 °C) probe positively biased in an oxygen plasma produced by a 500 μs electron beam.[10] As shown in the figure, standard laboratory power supplies produced significant variations in the measured probe currents. The fastest time response was seen in both battery-based power supplies, the series of five 9 V Energizer alkaline batteries (ER) and two Dynasty Power

Pack (Model PP12100) gel-cell batteries (GC). A Kepco bipolar power supply (Model BOP 100-1D) typically used in such experiments showed (curve K in Fig. 7) a slower response time than the batteries in sourcing and sinking the probe current. The slowest response in probe current was observed (curve HP in Fig. 7) when a Hewlett Packard dc power supply (Model 3611) was used as the voltage source.

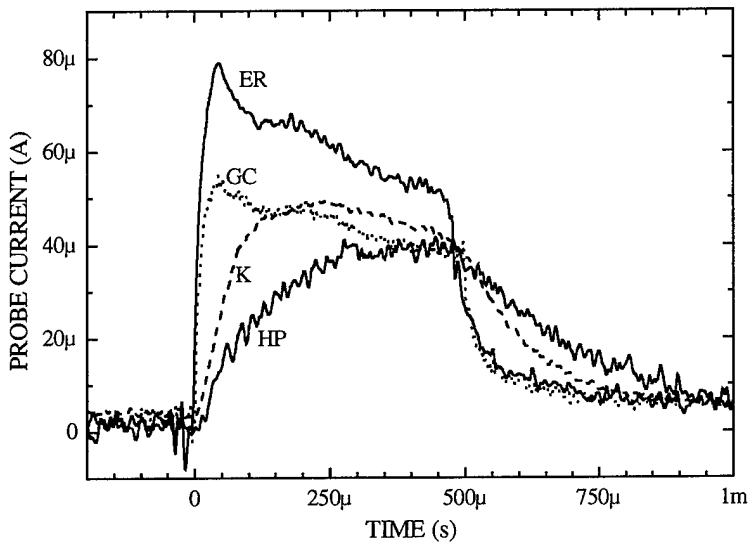

Figure 7 Temporally resolved electron currents to probe during and after a 500 μs e-beam pulse in oxygen background from various dc bias voltage sources: ER – five Energizer alkaline batteries (+45 V total); GC – two gel-cell batteries (+26 V total); K – Kepco BOP 100-1D bipolar dc power supply (set at +20 V); and HP – Hewlett Packard HP 3611 dc power supply (set at +20 V).

c. Data acquisition and analysis

An entire probe bias voltage sweep (±10 V, 0.05 V steps) can be carried out in 12-15 minutes, averaging over 20-50 shots per voltage step, with an e-beam repetition rate of 50 Hz. A series of the resultant I-V characteristics are shown in Fig. 8. For this data the probe was within the path of a 2 ms e-beam that was produced in a background of 75

mtorr argon. The output data file was 2.2 MB in size and consisted of 500 time divisions (10 μs/division) for each of the 400 voltage steps.

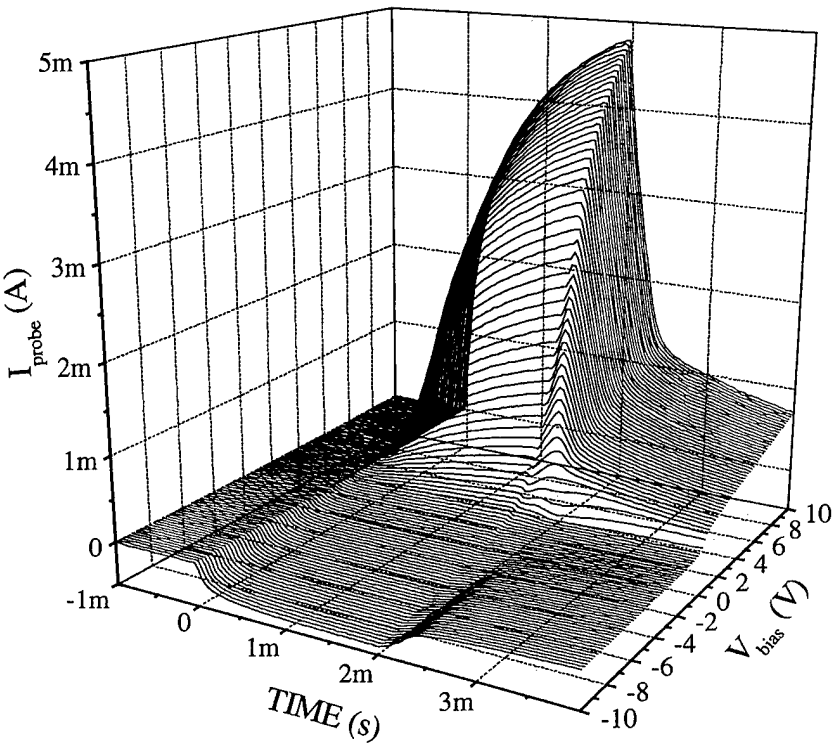

FIGURE 8 3D plot of temporally resolved I-V characteristics. 'Standard' I-V characteristics (as in Fig. 6) can be viewed by looking into the V_{bias} axis versus I_{probe}.

Data analysis was significantly streamlined by the batch analysis routine discussed in the previous section (Langmuir Analysis.vi). Manual determination of the plasma parameters from the data files could take multiple hours, depending on the time intervals of interest. Figure 9 shows the plasma parameters determined by both methods from the argon data shown in Fig. 8. The superimposed boxes are the plasma parameters

determined manually, with the height of the box representing error bars. The error bars were based on the range over the reported plasma parameters best fit the data.

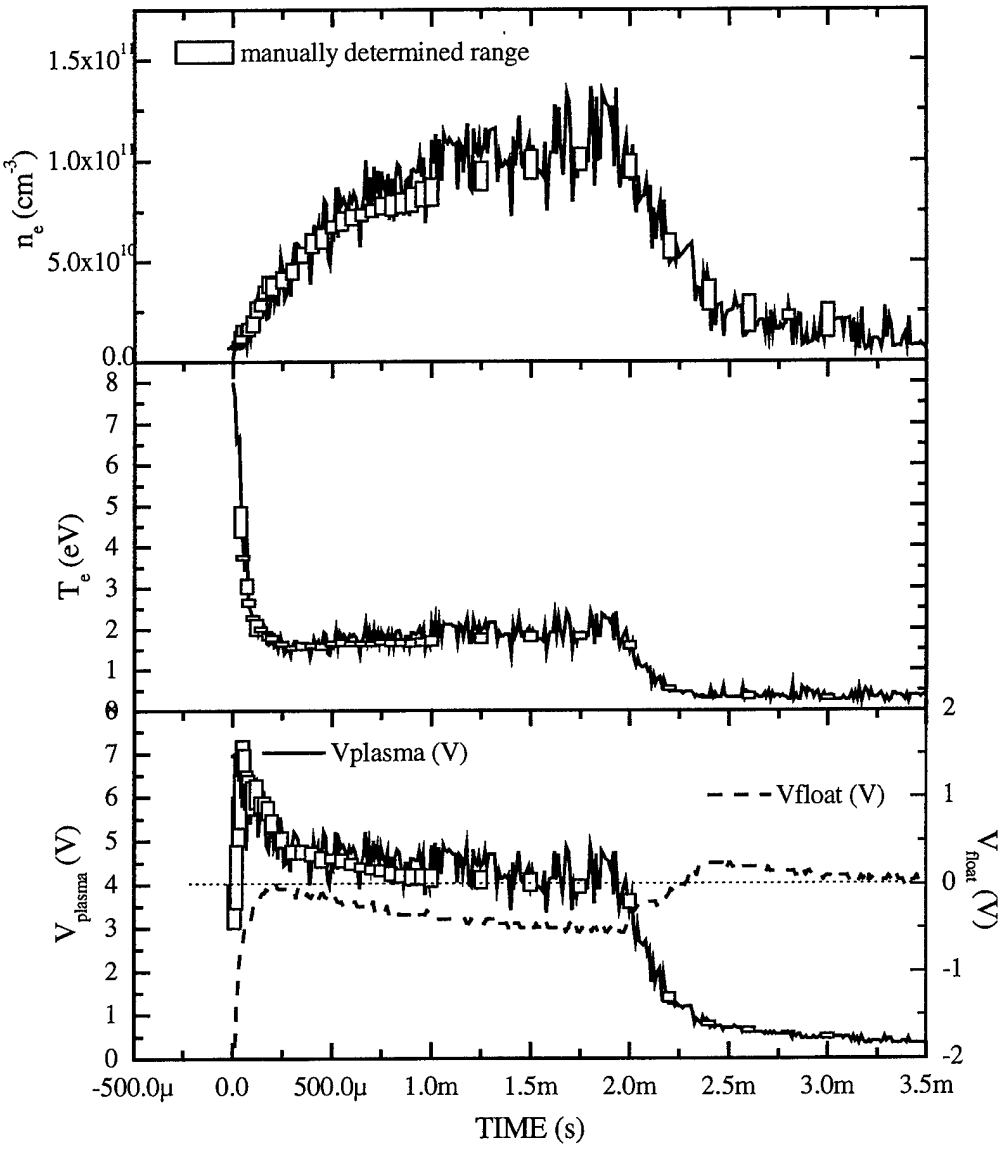

FIGURE 9 Results of probe data analysis from batch routine (black lines) and manual fitting routine (yellow boxes).

4. DISCUSSION

The probe design and construction materials presented here were fairly standard, although few groups have used an auxiliary heat source to maintain a clean probe surface. The observed probe contamination has been documented by a number of authors[11,12,13,14] and also modeled[15] in upper atmosphere applications. It should be stressed that in the present experiments, reproducible I-V characteristics were only obtained by heating the probe. A reasonable assumption would be that the probe surface remained constant in these experiments, although it may not have been necessarily 'clean', as it was not heated enough to glow. Typically to clean probes, a large negative or positive potential is applied so that ion or electron bombardment can remove the surface contamination layer. This process fails however if the time scale for recontamination is comparable to the time needed to acquire the I-V characteristic. Furthermore, even though the plasma densities were fairly high in these experiments, neither ion nor electron bombardment techniques could keep a consistent probe surface condition due to the modulated operation of the plasma source.

Although the exact thickness and composition of a contamination layer is typically undeterminable, from common vacuum practice it is well known that a monolayer per second is adsorbed on a surface at a pressure of 10^{-6} torr. Therefore even at high vacuum pressures (~ 10^{-6} torr), a clean probe surface significantly changes in just a few seconds. Specifically, in the presence of oxygen containing gases found in most vacuum systems (H_2O, O_2) a clean metal (i.e. tungsten) probe surface would rapidly oxidize. The high dielectric constant of an oxide layer ($\varepsilon \approx 80$) adds capacitance (0.1 – 1 μF) and a leakage current (comparable to a 10 - 100 kΩ bypass resistor) to the probe

circuit (see Reference 15 for a full mathematical treatment). Furthermore, the layer would not necessarily be constant for the duration of data collection, resulting in a large systematic error to the probe I-V characteristic, notably in the electron collection region. These errors may affect the determination of the electron temperature and the electron density from the electron saturation current, which should therefore be determined from the electron transition region as was done in these experiments. The I-V characteristics of Fig. 6 and analyzed results listed in Table I illustrate these changes. The I-V characteristics show a severe change in the location of the knee and the slope of the transition region (V_{plasma} and T_e, respectively) with temperature. The data suggests that the contaminants on the probe surface were being removed with the increasing probe temperature until a steady-state surface condition was achieved and consistent plasma parameters were found. At the highest temperature shown here (1.6 Amps), the increase in ion current and the poorer fit was likely due to a leakage current through the hot ceramic. Certainly, similar contamination issues will arise if the fill gas source is not of high purity, as the contamination rate increases directly with contaminant density. Thus, it is hard to imagine an application where probe contamination would not be an issue. Furthermore, it would be unrealistic to consider the probe 'clean' under these circumstances, but instead consistent in its surface composition and properties. Since contamination leads to overestimates of the electron temperature and underestimates of plasma density, the results reported here may represent upper and lower bounds of the electron temperature and plasma density, respectively.

For completion, two other issues associated with probe cleaning and contamination should also be discussed. First, with a continuous probe loop design, a

current could be run through the probe to similarly heat it. (This design is similar to a typical emissive probe[2], although the current is not large enough to permit electron emission.) However in this configuration, erroneous results may arise from the voltage drop across the probe element and/or secondary electron emission from the probe. The second issue is a further effect of probe contamination where a double-hump structure (DHS) appears in the I-V characteristic.[13] The DHS causes the I-V characteristic to appear as if there are two Maxwellian electron energy distributions in the system, due to the appearance of an additional knee and slope in the electron transition region. Stamate, *et al.*, further identified the presence of the DHS as the interaction between two adjacent probe sheaths, the second one due to a thin film of insulating material that had deposited on a portion of a [large planar] probe. The appearance of a DHS is not uncommon and was observed in some of the earlier experiments, but a systematic study was not within the scope of the present work.

The observed temporal dependencies due to the various probe bias supplies shown in Fig. 7 illustrate the necessity of *in situ* tests of support electronics as well as probe design. Alkaline batteries, which are typically used with a potentiometer as an inexpensive tunable voltage source, possessed a fairly rapid response time (< 10 μs) as did the gel-cell batteries. For the oxygen plasma used in those measurements, a rapid decay (≈ 50 μs) of the electron density was expected, due to electron-ion recombination once the ionization source (e-beam) was turned off. The two commercial dc power supplies however provided distorted current measurements due to what was initially believed to be inadequate slew rates. However, both of these commercial supplies have specifications below 50 μs recovery times. These slew rates/recovery times should have

demonstrated much faster responses then shown in Fig. 7, which implies there may have been additional capacitance and/or impedance mismatch (internal or external) associated with these power supplies that was not accounted for in the measurements. Nevertheless, an accurate representation of the physics was clearly masked by the use of these power supplies in the diagnostic; both the rapid turn-on and decay of the plasma electron current to the probe were distorted when they were used for the bias voltage source.

The application of electrostatic probes in magnetic fields has been discussed in the scientific literature and in a few review articles. In the absence of a magnetic field, OML theory uses Bohm diffusion to account for the ratio of electron to ion saturation current to a probe, $(I_e/I_i) = 28[\mu_{eff}]^{1/2}$, where μ_{eff} is the effective ion mass. The effective ion mass is derived from the dispersion relation for multiple ion species and is defined by $\mu_{eff}^{-1} \equiv \sum_s (n_{is}/n_{i\infty})/m_s$ where m_s is the mass of ion s, and $n_{is,\infty}$ are the density of ion s and the total ion density, respectively. In the presence of a magnetic field, the electrons move in helical orbits around the magnetic field lines due to the Lorentz force. The probe is only able to intersect a certain volume of the plasma electrons, specifically those confined to a magnetic flux tube with a radius comparable to the sum of the probe radius and electron gyroradius. (The electron gyroradius is given by $r_e \equiv m_e v_\perp / eB \Rightarrow r_e(cm) = 2.38[T_e(eV)]^{1/2}/B(G)$, where m_e is the electron mass, $v_\perp$ is the electron's velocity perpendicular to the magnetic field, e is the electron charge and B is the magnetic field strength.) For collisionless cases, the Sonmor-Laframboise model[16] was developed which showed a characteristic reduction of electron current and a weaker current dependence with bias voltage in the electron saturation region than OML theory. For collisional cases similar to the present conditions, Koo, *et al.*,[17] applied electron-

neutral collisions as the dominant diffusion mechanism over Bohm diffusion, both theoretically and experimentally. When electron-neutral collisions were considered, cross-field diffusion decreased the electron-to-ion saturation current ratio (I_e/I_I) by an additional factor proportional to $[T_e p]^{-1}$ where p is the neutral gas pressure (see Appendix B). Experimentally, a slightly weaker dependence was found than the electron-neutral collisional probe theory predicted, with impurity ion effects (unclear identification of μ_{eff}) being considered the dominant source of the observed discrepancy. Therefore, in the presence of a magnetic field, the saturation current ratio is expected to be less than predicted by the Bohm condition ($\approx$ 180) but more than predicted solely by cross field diffusion (20-60) in the 0.5 – 5 mtorr pressure range. In the present experiments, which operated in 150 - 165 Gauss magnetic fields and at 50 - 100 mtorr, I_e/I_i was crudely $\approx$ 10, as in Fig. 8. At this higher pressure range, the effects of electron-neutral collisions are expected to dominate the system, unlike the previous experiments. The more pronounced reduction of I_e/I_i by an order of magnitude in these experiments does follow the trend predicted by the cross-field diffusion theory of Koo: the relatively larger $[T_e p]$ value in these experiments (1.5 eV × 65 mtorr = 98) compared to the previous experiments (7.5 eV × 1 mtorr = 7.5) corresponded to a significantly larger decrease in I_e/I_i. The ion impurity effects are probably worse in the present experiments also, given the SF_6-based history of the chamber. Ideally, a broader pressure range in either experiment would provide a more complete quantitative test of the electron-neutral collisional probe theory.

The probe data (Fig. 8) and analysis (Fig. 9) show the response of the plasma electrons within the plasma active phase and afterglow. The electron temperature and plasma potential equilibrated rapidly after the ignition of the hollow cathode, although

the electron density continued to increase throughout the plasma's active phase. This temporal variation in electron density was primarily due to the plasma ions, which are highly collisional with the background gas (charge exchange mean free path $\approx$ 0.1 cm) and therefore not influenced by the magnetic field (ion gyroradius of $\approx$ 1 cm) and diffuse to the walls of the chamber. To maintain quasineutrality the plasma electrons must compensate for the diffusive loss of ions during the plasma pulse. Therefore the electron currents, which are preferentially lost along the magnetic field, adjust to match the ion density in the bulk plasma at all times. Thus, even though the plasma electrons possess very low temperatures and have small gyroradii ($\approx$ 0.02 cm) in the magnetic field, due to ambipolar diffusion they are only weakly confined by the magnetic field. Ambipolar diffusion also dominates particle flow in the afterglow where electron temperatures have dropped dramatically.

The low electron temperatures result in the low plasma potentials (< 6 Volt) and floating potentials (± 0.5 V) as shown in Fig. 9. The probe's negative floating potential during the active phase demonstrated the expected dominance of electron current. In the afterglow, the floating potential (and therefore current) became positive, on the same time scale of the plasma decay as the hotter electrons leave the system. The discrepancy in the results obtained using the batch process compared to the manual analysis in Fig. 9 were considered negligible, except in some of the electron density determinations. The plasma temperatures appeared to level out in the manually determined data, as opposed to the batch processed data that showed a slight increase throughout during the plasma active phase. This coincided with a minor increase in the plasma potential determined by the batch process, which was barely noticeable in Fig. 9. The first derivative of these later I-

V characteristics broadened slightly during the active phase, which resulted in a range of acceptable values for V_{plasma}. For the manually determined results, the best fits to the data were found to be slightly lower than the center of the first derivative peak, as chosen by the batch analysis routine. Also shown by the batch processed data, the plasma density was the most susceptible to minor changes in the other plasma parameters.

5. CONCLUSIONS

Due to the constantly changing environment in a modulated plasma, electrostatic Langmuir probe measurements required additional considerations not typically necessary in other applications. External heating of probes was believed to maintain a consistent surface condition for long periods of time, which in turn required robust construction materials (stainless steel and ceramic). A comparison of various laboratory power supplies in the probe circuitry showed various temporal performances in the probe data, some of which were dominated by the diagnostic itself instead of the physics of the system.

Due to the higher pressures and magnetic fields used in these plasmas, electron-neutral collisions significantly reduce the ratio of electron to ion saturation current seen in probe I-V characteristics. The plasma parameters determined from the probe data were found to be in excellent agreement between the batch and manual analysis techniques developed. More importantly, the results followed the basic physics associated with electron beam generated plasmas: low temperature, low field, high density plasma. With this active diagnostic system, much more information can be learned about these plasma systems, temporally and spatially.

ACKNOWLEDGEMENTS

The Office of Naval Research has supported this work.

APPENDIX A

MATERIALS USED IN LANGMUIR PROBE CONSTRUCTION

PROBE COMPONENT	TYPICAL DESCRIPTION	MANUFACTURER/ PART NUMBER
4-bore inner ceramic	1/16" OD rod with 1/64" bores	Omega Engineering, Inc. FRA-164116-6
Stainless steel ground shield	0.083" OD 0.063" ID	Small Parts, Inc. HTX-14-12
Outer ceramic sleeve	3/16" OD tube with 3/32" ID	Omega Engineering, Inc. ORA-332316-6
Heater wire	Rediohm 650; 0.010" diameter	Omega Engineering, Inc. 55730
Ceramic paste	Ceramic paste	Aremco, Inc. Ceramabond 509
BeCu pins	micropins	Allen Company HPR-40T/W

APPENDIX B

Koo, Hershkowitz and Sarfaty[17] derived the reduction of electron-to-ion saturation current as

$$[R] \propto \sqrt{T_e p}\left[I_1\left(\frac{1}{\sqrt{T_e p}}\right) \Big/ I_0\left(\frac{1}{\sqrt{T_e p}}\right)\right]$$

where T_e and p are the electron temperature and pressure, respectively, and I_v are the modified Bessel functions. Representing the Bessel functions in series form

$$I_v(x) = \sum_{s=o}^{\infty} \frac{1}{s!(s+v)!}\left(\frac{x}{2}\right)^{2s+v},$$

their expression can be written as

$$[R] \propto x^{-1}\left[\frac{\frac{x}{2} + \frac{1}{2}\left(\frac{x}{2}\right)^3 + \frac{1}{12}\left(\frac{x}{2}\right)^5}{1 + \left(\frac{x}{2}\right)^2 + \frac{1}{4}\left(\frac{x}{2}\right)^4}\right]$$

where $x = [T_e p]^{-1/2}$. Factoring out (x/2) from the numerator and only keeping up to second order terms in x, the expression becomes

$$[R] \propto \frac{1}{2}\left[\frac{1 + \frac{1}{2}\left(\frac{x}{2}\right)^2}{1 + \left(\frac{x}{2}\right)^2}\right].$$

Taylor expanding the denominator then yields

$$[R] \propto \frac{1}{2}\left(1 - \frac{x^2}{8}\right) \rightarrow \frac{1}{2} - \frac{1}{16 T_e p},$$

which provides the $[T_e p]^{-1}$ dependence quoted in the text.

REFERENCES

[1] I. Langmuir, in Collected Works of Irving Langmuir, edited by G. Suits (Pergamon, New York, 1961), Vol. 5.

[2] N. Hershkowitz, in Plasma Diagnostics: Discharge Parameters and Chemistry, edited by D. M. Manos and D. L. Flamm (Academic Press, New York, 1989), Chapter 3.

[3] F. F. Chen, in Plasma Diagnostic Techniques, edited by R. H. Huddlestone and S. L. Leonard (Academic Press, New York, 1965), Chapter 4.

[4] See also an undergraduate laboratory manual at http:\\www.physics.ucla.edu/plasma~exp/180E-W97/notes.html.

[5] The Debye length is given by $[\varepsilon_0 T_e/n_e e^2]^{1/2}$ where the symbols have their usual designations. For more rapid computation, this expression can be simplified to $\lambda_D(\text{cm}) = 743[T_e(\text{eV})/n_e(\text{cm}^{-3})]^{1/2}$.

[6] Burr-Brown precision low-cost isolation amplifier ISO122. The ISO122 amplifier allowed a differential current measurement, which improved the S/N of the signal. By design, the ISO122 amplifier modulates the signal at a 500 kHz duty cycle across an isolation barrier. Consequently, there is a residual 500 kHz demodulation ripple at the output. From the manufacturer's specifications, the ISO122 possesses a 50kHz signal bandwidth and 0.020% maximum nonlinearity with a fixed unity gain under these conditions.

[7] See Burr-Brown Application Bulletin SBOA012, *"Simple output filter eliminates ISO amp output ripple and keeps full bandwidth,"* by M. Stitt (1991).

[8] See experiments DL7-119/129/134/154, DL8-19 and DL12-110 for additional discussion and construction of heated langmuir probes.

[9] See DL14-15 (010531.opj).

[10] See DL8-143 (000207\supply test.opj).

[11] W. E. Amatucci, M. E. Koepke, T. E. Sheridan, M. J. Alport, and J. J. Carroll, *Rev. Sci. Instrum.* **64**, 1253 (1993).

[12] S. Laubé, T. Mostefaoui, and B. Rowe, *Rev. Sci. Instrum.* **71**, 519 (2000).

[13] W. E. Amatucci, P. W. Schuck, D. N. Walker, P. M. Kinter, S. Powell, B. Holback, and D. Leonhardt, *Rev. Sci. Instrum.* **72**, 2052 (2001).

[14] E. Stamate and K. Ohe, *J. Vac. Sci. Technol.* **20**, 661 (2002).

[15] A. Piel, M. Hirt, and C. T. Steigies, *J. Phys. D* **34**, 2643 (2001).

[16] L. J. Sonmor and J. G. Laframboise, *Phys. Fluids B* **86**, 2472 (1991).

[17] B.-W. Koo, N. Hershkowitz, and M. Sarfaty, *J. Appl. Phys.* **86**, 1213 (1999).